https://doi.org/10.5194/acp-2022-478
Preprint. Discussion started: 28 July 2022

Atmospheric Chemistry and Physics Discussions

High variations of BVOC emissions from Norway spruce in boreal forests

Hannele Hakola[1], Ditte Taipale[2,3], Arnaud Praplan[1], Simon Schallhart[1], Steven Thomas[1], Toni Tykkä[1], Aku Helin[4], Jaana Bäck[5], Heidi Hellén[1]

[1]Atmospheric Composition Research, Finnish Meteorological Institute, FI-00101 Helsinki, Finland
[2]Kilpisjärvi Biological Station, Faculty of Biological and Environmental Sciences, Käsivarrentie 14622, 99490 Kilpisjärvi, Finland
[3]Institute for Atmospheric and Earth System Research/Physics, Faculty of Science, University of Helsinki, P.O. Box 64, 00014 Helsinki, Finland
[4] Finnish Institute of Occupational Health, P.O. Box 40, FI-00032 Työterveyslaitos, Finland.
[5] Institute for Atmospheric and Earth System Research/Faculty of Agriculture and Forestry, University of Helsinki, PO Box 27, 00014, Helsinki, Finland

Correspondence to: Hannele Hakola (hannele.hakola@fmi.fi)

Abstract

The biogenic volatile organic compound (BVOC) emission rates of Norway spruces published vary a lot. In this study we combined published Norway spruce emission rates measured in boreal forests (Meeningen et al., 2017; Bourtsoukidis et al., 2014a, 2014b; Hakola et al., (2003, 2019)) and added our new, unpublished emission data from southern (SF) and northern Finland (NF). Standardized summer monthly mean emission potentials of isoprene vary from below detection limit to 7 µg $g^{-1}_{(dw)}$ h^{-1}, and monoterpene (MT) and sesquiterpene (SQT) emission potentials 0.01–3 µg $g^{-1}_{(dw)}$ h^{-1} and 0.03-2.7 µg $g^{-1}_{(dw)}$ h^{-1}, respectively. In this study, we found much higher SQT emissions from Norway spruces than measured before and on average SQTs had higher emission potentials than isoprene or MTs. The highest monthly mean SQT emission potential 13.6 µg $g^{-1}_{(dw)}$ h^{-1} was observed in September in southern Finland.

We found that none of the younger (33-40 years) trees in Hyytiälä, southern Finland, emitted isoprene, while one 50-year-old tree was a strong isoprene emitter. However, this could not be confirmed at other sites since all measured small trees were growing in Hyytiälä, so this could also be due to the same genetic origin. On average, older trees (>80 years) emitted about ten times more isoprene and MTs than younger ones (<80 years), but no clear difference was seen in SQT emissions. SQT emissions can be more related to stress effects.

As shown here for Norway spruce, it is possible that the emission factor of SQTs is significantly higher than what is currently used in models, which may have significant effects on the prediction of formation and growht of new particles, since the secondary organic aerosol (SOA) formation potential of SQTs is high and this may have significant effects on the formation and growth of new particles. Due to high secondary organic aerosol (SOA) formation potentials of SQTs the impact on SOA formation and mass could be even higher.

https://doi.org/10.5194/acp-2022-478
Preprint. Discussion started: 28 July 2022

1. Introduction

The boreal forest covers about $11 \cdot 10^6$ km^2 i.e. about 30 % of the global forest (Pan et al., 2013). The amount of tree species is not very diverse, consisting mainly of conifers such as pines and spruces and larch species especially in eastern part of Russian boreal forest (Soja et al., 2007). Some broadleaved deciduous trees are also common and include e.g. Betula sp., Alnus sp. and Populus sp. The terrestrial vegetation, mainly trees, emit large amounts of volatile organic compounds (VOCs) to the atmosphere impacting the formation of ozone, secondary organic aerosol and clouds. These biogenic emissions (BVOC) dominate global VOC emissions consisting mainly of isoprene (ISOP), monoterpenes (MT), sesquiterpenes (SQT), methanol and acetone (Sindelarova et al., 2014). During the last decade the new technique to measure atmospheric total hydroxyl radical (OH) reactivity has been introduced to describe the VOC content of the air. By measuring how much OH radicals are consumed in the reactions and comparing this amount with the measurements of everything we know that reacts in the air with OH radicals, we can evaluate how much unknown reactive compounds are in the atmosphere. Total OH reactivity studies have shown that there are lots of unknown reactivity especially in the air of boreal forests (Yang et al. 2016). This reactivity is not explained by the traditionally measured BVOCs, their oxidation products or other known reactive compounds (e.g. CO, CH_4, NO_x, O_3) (e.g. Praplan et al., 2019). A significant fraction of the unknown reactivity has also been found directly in the emissions of boreal trees (Nölscher et al. 2013 and Praplan et al. 2020). Therefore, more studies on BVOC emissions are needed to better understand biosphere-atmosphere interactions.

Especially ISOP and MT have been studied quite intensively during past decades in boreal areas and MTs have been found to dominate ISOP emissions (e.g., Artaxo et al., 2022; Rinne et al., 2009). There are much more studies on MT and ISOP emissions than SQTs in the boreal area and the few existing studies show that SQT emissions can be substantial (e.g., Bourtsoukidis et al., 2014 a,b; Hakola et al., 2001, 2006, 2017; Hellén et al., 2020, 2021; Schallhart et al., 2018). SQT emissions, especially β-farnesene, are often related to biotic stresses and therefore the emissions can be highly variable depending on the stress factors (Petterson, 2007; Kännaste et al., 2008; Niinemets, 2010; Joutsensaari et al., 2015; Matsui and Koeduka, 2016).

Emission potentials and compound composition vary a lot between different tree species (Karl et al., 2009), but there are also large variations in the emission between different individuals of the same tree species. For example, Bäck et al. (2012) showed that Scots pine trees of the same age, growing in the same environment, emit very different monoterpene selections. This has also been found to be true in the emissions of Norway spruce (Hakola et al., 2017). When considering the atmospheric impact of biogenic emissions, it is essential to know the species-specific composition of the emission, because for example atmospheric reactivity and aerosol formation potential of different compounds varies a lot (e.g. Hellén et al., 2018). Since emission rate and composition within the same tree species is so variable, we collected all available data of Norway spruce that could be used for emission potential calculations to investigate if e.g. growing location or age of a tree could explain the variations. In addition to the published data, we present new data from Hyytiälä, southern Finland from 2019 and 2021 and Pallas, northern Finland, from 2020.

To demonstrate the consequences of emission group selection in new particle formation, we used this newly measured emission data to model aerosol formation and growth in two different environments, southern boreal forest in Finland and a sub-Arctic forest in Finnish Lapland. As a comparison, we simulated the aerosol processes with emissions from MEGAN v 2.1 model

https://doi.org/10.5194/acp-2022-478
Preprint. Discussion started: 28 July 2022

(Model of Emissions of Gases and Aerosols from Nature). MEGAN2.1 is a modeling framework for estimating fluxes of biogenic compounds between terrestrial ecosystems and the atmosphere and utilizes standardized emission potentials from specific plant functional types to characterize the emissions (Guenther et al, 2012). Our simulations with real data thus provide a 'reality check' for the tabulated emission potential approach.

2. Experimental

1.1. Measurement sites and earlier emission measurements

The measurements were conducted in a southern boreal forest in Hyytiälä (hereafter called Southern Finland, SF) and in a northern boreal Norway spruce forest, at Pallas, Kenttärova (hereafter called Northern Finland, NF). The measurement times and the tree ages are given in Table 2.

The NF site (Pallas Kenttärova, 67.59°N, 24.15°E) lies on a hilltop plateau at an elevation of 347 m a.s.l.. It is a sub-Arctic site which is characterized by the very short and intense growing season. Forests at these kind of sub-Arctic areas are sparse and the average tree height is much lower than at the more southern boreal forests. At Pallas site in 2021, the age of the trees varied from 90 to 250 years. The site is described in detail in Lohila et al. (2015) and in Aurela et al. (2015).

We measured altogether three mature spruces. The continuous analyses were conducted in a container about 2 m from the in-situ measured tree (Fig. 1). In addition to in-situ measurements, we also measured campaign-wise two trees growing near the container off-line; one growing by a small forest road shown in Fig. 1 and the other growing deeper in the forest. These off-line measurements included only present year's new growth.

The SF site (SMEAR II station in Hyytiälä, Station for Measuring Forest Ecosystem-Atmosphere Relations, 61.51° N, 24.18° E, 181 m a.s.l.) is described in Hari and Kulmala (2005). The vegetation consists of a rather homogeneous Scots pine forest with some birches and Norway spruces growing in a mixture or understorey. The instrument was located in a container in a clearing in the forest (Fig. 2). The measured trees are marked on Fig. 2 and the approximate ages tabulated in Table 2.

The data include earlier measurements from 2011, 2014 and 2015 that has been published in Hakola et al. (2017) and new measurements from 2019 and 2021. In 2021, the measurements covered two different trees. One of the trees was the same one as measured in 2011, because we wanted to see if the age of the tree would affect its emissions. The other tree measured in 2021 was growing deeper in the forest (ca. 15 m tall, 50 years old, Fig. 2). This tree was measured using adsorbent tubes, because the big tree was growing too far from the container to be measured with on-line gas-chromatograph-mass-spectrometer (GC-MS). With this tree we wanted to see if a big tree would emit differently than smaller ones growing close to the container. The ages of the trees and measurement times are shown in Table 2 and they are named as NF/SF and the year of the measurements.

https://doi.org/10.5194/acp-2022-478
Preprint. Discussion started: 28 July 2022

In addition to the Hyytiälä and Pallas data, two older data sets are also included in the analysis. Data acquired in Sodankylä (67.25°N, 26.36°E), northern Finland, and Järvenpää (60.28°N, 25.52°E), southern Finland (Hakola et al., 2003). These datasets are named as NF2 2002 and SF2 2001.

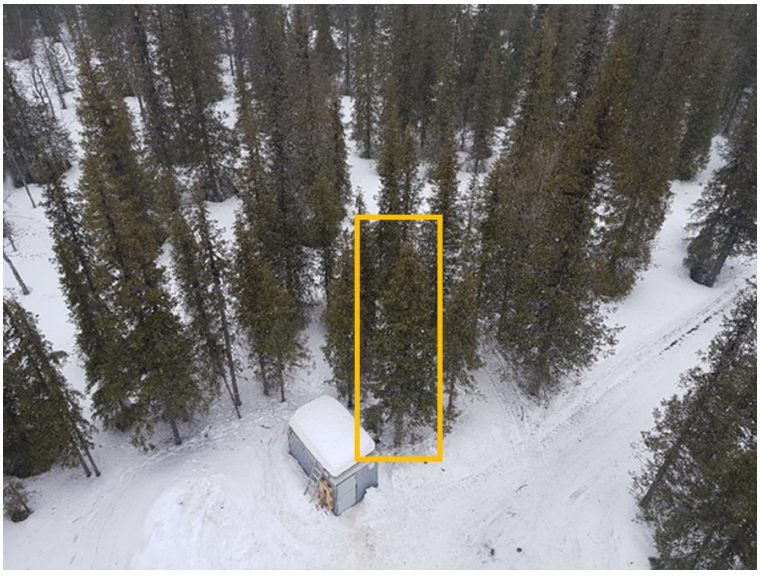

Figure 1: Measurement container at Pallas, Kenttärova site. The continuously measured tree was the closest to the container.

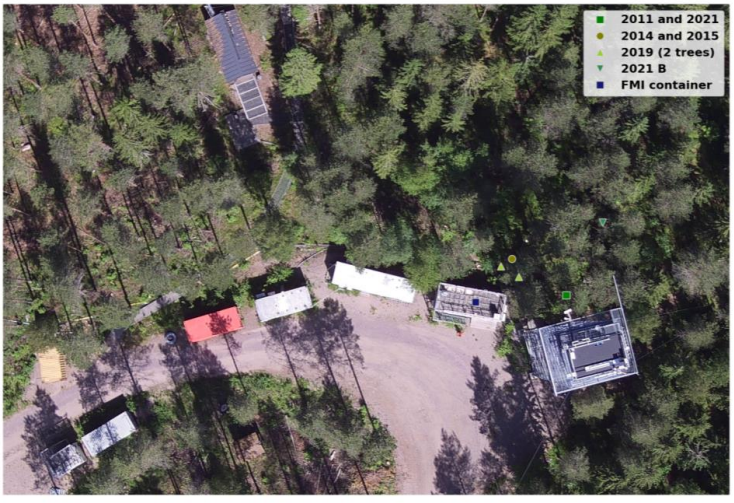

Figure 2: Measurement site in Hyytiälä with the measured Norway spruce trees marked. Picture: Pavel Alekseychik (National Resources Institute Finland), using a camera Zenmuse XT2 (RGB sensor) on a Drone Matrice 210 V2.

https://doi.org/10.5194/acp-2022-478
Preprint. Discussion started: 28 July 2022

2.1. New, unpublished emission measurements

The emission measurement setup used in these campaigns has been described in detail previously in e.g. Hakola et al. (2017). Briefly, the measurements used a branch enclosure consisting of a ca. 6 L fluorinated ethylene propylene (FEP) dynamic chamber, which was flushed with 3-6 L min^{-1} of humidified zero air generated by a commercial catalytic converter (HPZA-7000, Parker Hannifin Corporation). Two custom-built data loggers were used during the campaigns. The set-up consisted of a thermistor (Philips KTY 80/110, Royal Philips Electronics, Amsterdam, Netherlands) for the temperature inside the chamber and a quantum sensor (LI-190SZ, LI-COR, Biosciences, Lincoln, USA) for the photosynthetically active radiation (PAR), measured just above the enclosure.

On-line measurements/in situ analysis was performed using a thermal desorption - gas chromatograph - mass spectrometer (TD-GC-MS) (a thermal desorption unit Turbo Matrix 350, a gas chromatograph Clarus 680 and a mass spectrometer Clarus SQ8 T, all manufactured by Perkin-Elmer, Inc. Waltham MA, U.S.A.). It was connected to the chamber via a 7 m long, 3.2 mm (i.d.) tubing heated few degrees above the ambient temperature and pumped with 0.5 – 2.0 L min^{-1} make up flow, followed by 2.5 m long, 1.59 mm (i.d.) tube, with a flow of 40 mL min^{-1}. All tubing was made of FEP. The VOC samples were collected directly into a cold trap filled with Tenax TA (50 %) and Carbopack B (50 %) of the TD-GC-MS for 30 min every hour or every second hour. The trap was kept at 20-25ºC during sampling to prevent water vapour present in the air from accumulating in the trap. A DB-5MS column (60 m; i.d., 0.25 mm; film thickness, 0.25 µm from Agilent Technologies, Santa Clara CA, U.S.A.) was used for the separation. The column was kept 2 min at 60ºC and then heated at the rate of 8ºC min^{-1} to 270ºC where it was kept for 2 min. The total time of the analysis was 30.25 min.

Helin et al. (2020) detected significant losses of β-farnesene within our in-situ TD-GC-MSs, which have been used in earlier studies of Norway spruce emissions (Hakola et al., 2017). For the new measurement campaigns conducted in 2019-2021 and presented here, the instrument was modified by changing the stainless steel lines in the online sampling box of the TD unit into FEP tubing and by using an empty Silcosteel sorbent tube instead of an empty stainless steel sorbent tube in the sample path of the TD unit. This increased the recovery of β-farnesene from ~10 % to >80 %.

Additional offline samples taken in Hyytiälä in 2021 and in Pallas in 2020 and also two previous datasets (NF2 2002 and SF2 2001) were acquired using Tenax TA/Carbopack B adsorbent tubes with the same method. The sampling flow was ~100 and ~200 ml min^{-1} at Hyytiälä and in Pallas, respectively, and the sampling time was 30 min. The adsorbent tube samples, which were stored at 4°C until analysis, were analysed later in the laboratory of the Finnish Meteorological Institute using an automatic TD unit (TurboMatrix 350) connected to a GC (GC, Clarus 680) coupled to a quadrupole MS (MS, Clarus SQ 8 T), all purchased from PerkinElmer, Inc. (Waltham, MA, USA). This offline TD-GC-MS method is comparable to the online method (see e.g. Helin et al., 2020).

A four-point calibration was performed using liquid standards in methanol solutions for both on- and off-line measurements. Standard solutions (5 µl) were injected onto adsorbent tubes and then flushed with nitrogen (80-100 mL min^{-1}) for 10 min to remove the methanol. The calibration solution included the following MTs: α-pinene, camphene, β-pinene, 3Δ-carene, p-cymene, 1,8-cineol, limonene, myrcene, terpinolene and linalool and the following SQTs: longicyclene, iso-longifolene, β-caryophyllene, β-farnesene and α-humulene. Unknown

https://doi.org/10.5194/acp-2022-478
Preprint. Discussion started: 28 July 2022

sesquiterpenes were tentatively identified based on the comparison of the mass spectra and retention indexes (RIs) with NIST mass spectral library (NIST/EPA/NIH Mass Spectral Library, version 2.0). RIs were calculated for all SQTs using RIs of known SQTs and MTs as reference. These tentatively identified SQTs were quantified using response factors of calibrated SQTs having the closest mass spectra resemblance. Isoprene was calibrated using gaseous standard (National Physical Laboratory, 32 VOC mix at 4 ppb level or terpene mix at 2 ppbv level).

2.3 Emission rate and potential calculations

The emission rate (E) is determined as the mass of compound per needle dry weight and per time according to

$$E = \frac{(C_2 - C_1)F}{m} \quad (1)$$

Here C_2 is the concentration in the outgoing air, C_1 is the concentration in the incoming air, and F is the flow rate into the enclosure. The dry weight of the foliage mass (m) was determined by drying the needles and shoot from the enclosure at 75 ºC for 24 hours.

A strong dependence of biogenic VOC emissions on temperature has been seen in emission studies of ISOP, MTs, and SQTs (e.g. Hellén et al., 2021). The temperature dependent emission potentials for MTs and SQTs were calculated according to Guenther et al. (1993) and isoprene emission potentials were calculated using the temperature and light dependent algorithm according to Guenther et al. (2012).

2.4 Modelling impact of VOC emissions on aerosol formation and growth

Simulations were conducted using the model presented in Taipale et al. (2021). This model includes modules for emissions of VOCs from stress-free and stressed trees, boundary layer meteorology, atmospheric chemistry, and aerosol formation and growth. Certain parts of the model setup used in this study are different from the setup described in Taipale et al. (2021).

2.4.1 Plant emissions of volatile organic compounds

In this study, the emissions (E_i, µg m^{-2} h^{-1}) of MTs and SQTs (i) were modelled as:

$$E_i = \varepsilon_i * LAI * \gamma_i, \quad (2)$$

where ε_i (µg m^{-2} h^{-1}) is the emission potential of i, LAI (m^2 m^{-2}) is the one-sided leaf area index, and γ_i (unit-less) is an activity factor which accounts for changes in standard temperature conditions (Guenther et al., 1993):

$$\gamma_i = \exp(\beta_i * (T - T_s)) \quad (3)$$

where T is temperature (°C), T_s is the standard temperature (30 °C), and β_i is 0.1 °C^{-1} and 0.17 °C^{-1} for monoterpenes and sesquiterpenes, respectively (Guenther et al., 2012).

https://doi.org/10.5194/acp-2022-478
Preprint. Discussion started: 28 July 2022

2.4.2 Environmental conditions and atmospheric chemistry

The model was constrained by environmental and atmospheric values observed in Hyytiälä (southern Finland, SF), as well as Pallas and Värriö, (northern Finland, NF), due to data availability (Fig. 3). The aim was to use reasonable values and not simulate one specific year or location. The one-sided leaf area index of Norway spruce forest stands was fixed to 6.0 m^2 m^{-2} (Kalliokoski et al., 2020) and 3.3 m^2 m^{-2} (Thum et al., 2008) for southern Finland and Finnish Lapland, respectively. In the simulations the concentration of ozone (O_3) was kept constant throughout the day. For simulations of Lapland, we used monthly median year 2020 O_3 concentration data from Pallas Sammaltunturi obtained via EBAS. These values are almost identical to observations from SMEAR I, Värriö, during the same time period (http://urn.fi/urn:nbn:fi:att:8b3c67b4-22c0-4589-be00-a3d0341064d5). For simulations of southern Finland, we used monthly median year 2020 O_3 concentration data from SMEAR II, measured at 16.8 m (https://doi.org/10.23729/62f7ad2c-7fe0-4f66-b0a4-8d57c80524ec). For simulations of both environments we calculated the monthly median of daily maximum OH concentration using the proxy presented by Petäjä et al. (2009) and year 2020 observed UVB radiation from the SMEAR I (http://urn.fi/urn:nbn:fi:att:8b3c67b4-22c0-4589-be00-a3d0341064d5) and SMEAR II (https://doi.org/10.23729/62f7ad2c-7fe0-4f66-b0a4-8d57c80524ec) stations, respectively. These daily maximum OH concentrations were used as input to the model, and the concentration of OH then decreased in the model as a function of a decrease in available solar light. We used daily maximum sulfuric acid (H_2SO_4) concentrations reported by Kyrö et al. (2014) and Asmi et al. (2011) from Lapland, and by Petäjä et al. (2009) from southern Finland, as input to the model, and let the concentration of sulfuric acid decrease as a function of a decrease in solar light. In the simulations, the condensation sink (CS) was kept constant throughout the day. For simulations of Lapland, we used CS data from Vana et al. (2016), Asmi et al. (2011) and Komppula et al. (2006), while we used CS data from Vana et al. (2016) for simulations of southern Finland. For simplicity, the daily modelled temperature pattern followed that of the solar zenith angle with a forward shift of 1 h. For simulations of both environments, we used the monthly median of daily maximum and minimum temperatures measured at 15 m (Lapland) and 16.8 m (southern Finland) during the year 2020 at the SMEAR I (http://urn.fi/urn:nbn:fi:att:8b3c67b4-22c0-4589-be00-a3d0341064d5) and SMEAR II (https://doi.org/10.23729/62f7ad2c-7fe0-4f66-b0a4-8d57c80524ec) stations. For simulations of both environments, we used the monthly median of daily maximum year 2020 ERA5 reanalysis boundary layer height retrieved for the grid cells closest to Pallas and Hyytiälä, respectively. These maximum values were downscaled by 25 % since one fixed value was used for the whole day.

https://doi.org/10.5194/acp-2022-478
Preprint. Discussion started: 28 July 2022

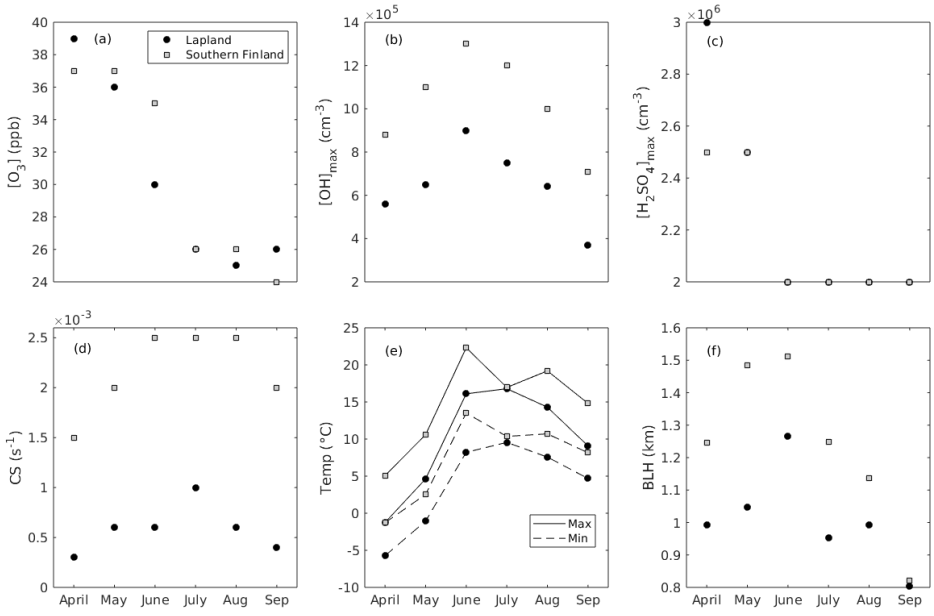

Figure 3. Model input. (a) Ozone concentration. (b) Daily maximum OH concentration. (c) Daily maximum sulfuric acid concentration. (d) Condensation sink. (e) Daily maximum and minimum temperatures. (f) Planetary boundary layer height (BLH).

The following chemical reactions were included in the model:

$OH + MTs \rightarrow products + \gamma OxOrg_{(g)}$ (R1)
$O_3 + MTs \rightarrow products + \gamma OxOrg_{(g)}$ (R2)
$O_3 + SQTs \rightarrow products + \gamma OxOrg_{(g)}$ (R3)
$OxOrg_{(g)} \rightarrow OxOrg_{(p)}$ (R4)
$OH + SO_2 \rightarrow H_2SO_{4(g)}$ (R5)
$H_2SO_{4(g)} \rightarrow H_2SO_{4(p)}$ (R6)

where T is temperature (K), p indicates particle phase, g indicates gas phase, and OxOrg is the sum of all organic compounds which contribute to aerosol processes. Reaction rates for each reaction are summarized in Table 1. Reactions with NO_3 were omitted, because simulations were only conducted for daytime conditions.

Table 1: Reaction rates and yields for the reactions 1-6. CS is the condensation sink.

Reaction	Reaction rate	Yield (%)
R1	$1.2 \cdot 10^{-11} \cdot e^{(440/T)}$ ($cm^3 \cdot molecule^{-1} \cdot s^{-1}$)	1.7
R2	$8.05 \cdot 10^{-16} \cdot e^{(-640/T)}$ ($cm^3 \cdot molecule^{-1} \cdot s^{-1}$)	5.0
R3	$1.2 \cdot 10^{-14}$ ($cm^3 \cdot molecule^{-1} \cdot s^{-1}$)	7.7
R4	CS·0.5	
R5	$1.5 \cdot 10^{-12}$ ($cm^3 \cdot molecule^{-1} \cdot s^{-1}$)	
R6	CS	

https://doi.org/10.5194/acp-2022-478
Preprint. Discussion started: 28 July 2022

Some VOCs, and especially VOCs with endocyclic double bonds, can undergo autoxidation (Crounse et al., 2013; Ehn et al., 2014) whereby compounds with low volatility and high molecular mass (HOM: highly oxygenated organic molecules) are formed (e.g., Ehn et al., 2012, 2014; Jokinen et al., 2015; Berndt et al., 2016; Kurtén et al., 2016; Bianchi et al., 2019; Zhao et al., 2020). These highly oxygenated organic molecules have been found to be a major component of secondary organic aerosol (e.g. Ehn et al., 2014; Mutzel et al., 2015; Tröstl et al., 2016; Roldin et al., 2019). The yields by which HOM are formed are specific for individual parent molecules and isomers (e.g., Ehn et al., 2014; Bianchi et al., 2019), but they also depend on the blend of atmospheric molecules, including VOCs (McFiggans et al., 2019). Since HOM yields have, until now, only been determined for a very limited selection of VOCs, and since no algorithm to quantify how the concentration blend affects HOM yields have been proposed so far, mono- and sesquiterpenes were treated as groups of compounds in the model. Thus, in R1-3, γ is either the reported HOM yield, as defined in Ehn et al. (2014), or the reported SOA yield divided by 2.2 to account for the fact that SOA yields represent mass yields, and not molar yields as it is the case of HOM yields. γ_1 is based on Jokinen et al. (2015) and Berndt et al. (2016), γ_2 is based on Jokinen et al. (2015) and Ehn et al. (2014), while γ_3 is based on Mentel et al. (2013).

2.4.3 Formation and growth of new particles

Clustering and activation of new atmospheric aerosol particles was calculated as (Paasonen et al., 2010):

$$J_2=\alpha_1 * [H_2SO_4]^2 + \alpha_2 * [H_2SO_4]\,[OxOrg] + \alpha_3 * [OxOrg]^2 \quad (4)$$

where J_2 ($cm^{-3}\,s^{-1}$) is the formation rate of neutral 2 nm sized clusters, and $\alpha_{1\text{-}3}$ are coefficients (Table 3 in Paasonen et al., 2010). For simplicity, only one growing aerosol mode was considered, and a unit-less correction term (KK), which determines how large a fraction of the activated clusters reaches the growing mode, was therefore included (Kerminen and Kulmala, 2002):

$$KK=\exp(\eta * [1/D_p-1/D_{clus}]) \quad (5)$$

where D_p and D_{clus} are the diameters of the growing mode and clusters, respectively, and η (nm) is (Kerminen and Kulmala, 2002):

$$\eta = 1830\ nm^2 s\ h^{-1} * CS/GR \quad (6)$$

where CS is the condensation sink and GR (nm h^{-1}) is the condensational particle diameter growth rate. The growth rate of newly formed 2-3 nm particles was calculated as (Nieminen et al., 2010):

$$GR_{2\text{-}3\ nm}=0.5\ nm\ h^{-1} * CC \times 10^{-7}\ cm^3 \quad (7)$$

where CC is the concentration of condensable vapours which was assumed to be the sum of sulfuric acid and OxOrg, and where it was assumed that the molar mass of OxOrg are 3.5 times larger than that of sulfuric acid (Ehn et al., 2014):

https://doi.org/10.5194/acp-2022-478
Preprint. Discussion started: 28 July 2022

$$CC=[H2SO4]+[OxOrg] * 3.5^{1/3} \quad (8)$$

The strong dependency of particle growth rates on particle size, which has been observed in field conditions (Hirsikko et al., 2005; Yli-Juuti et al., 2011; Häkkinen et al., 2013), was also accounted for (Hirsikko et al., 2005; Yli-Juuti et al., 2011):

$$GR_{3\text{-}7\ nm}=2 * GR_{2\text{-}3\ nm} \quad (9)$$
$$GR_{>7}\ nm=2.3 * GR_{2\text{-}3\ nm} \quad (10)$$

The increase in the diameter of the growing mode was defined by the growth rate:

$$\Delta D_p/\Delta t=GR/3600\ s\ h^{-1} \quad (11)$$

while the increase in the number of new particles (Np, cm^{-3}) was determined by the formation of new particles which reaches the growing mode and the coagulation of particles in the growing mode:

$$\Delta Np/\Delta t=J_2 * KK - CoagS * Np \quad (12)$$

where the coagulation sink (CoagS, s^{-1}) was calculated as (Lehtinen et al., 2007):

$$CoagS=CS * (0.71\ nm/D_p)^{1.6} \quad (13)$$

3. Results

3.1 Previously unpublished emission rates

The full time series of unpublished Norway spruce emission rates of MTs, oxygenated monoterpenoids (OMTs; linalool, 1,8-cineol, and bornylacetate) and SQTs are shown in Fig. A1 and isoprene and MBO emission rates in Fig. A2 (Appendix 1). Calculated monthly mean emission potentials (30°C) are presented in Table 2 together with previously published data that will be reviewed in Sect. 4. The approximate ages of the trees are shown in Table 2.

3.1.1 Emission rates at the boreal forest site in Hyytiälä, southern Finland

In 2019, emissions from a small tree (SF 2019) were measured during the growing season. It emitted only small amounts of ISOP, and MT and SQT emissions were generally lower than in the previously reported Norway spruce emissions (Hakola et al., 2003). The statistics of the daily mean emission rates are shown in Fig. 4. Figure 5 shows the mean diurnal variations during summer months. Diurnal variation of the emission rates followed the variation of the temperature being highest in the afternoon and very low or below detection limits during the night. Isoprene emission rates were very low all the time. MTs were the dominant group in the emissions in July, but also SQT were important throughout summer.

The tree measured in Hyytiälä in 2021 (SF 2021) was the same one that was measured in 2011 (SF 2011). In 2011, the SQT measurements were not reliable, but otherwise the results remained similar after ten years with very low ISOP, MT and OMT emission potentials (Table 2). The comparison between the years is difficult since the measurements are not from the same periods in 2011 and 2021. In 2021 the measurements were conducted late summer in August, whereas in 2011 in spring/early summer. Based on these measurements, the aging of the tree

https://doi.org/10.5194/acp-2022-478
Preprint. Discussion started: 28 July 2022

did not affect the emissions at least not yet on this ten years period. In 2021, an additional big tree growing deeper in the forest was measured (SF 2021B) for comparison. The big tree (SF 2021B) emitted isoprene with much higher rate than the small trees (mean 1498 ng g_{dw}^{-1} h^{-1}) and also MT emission rates (mean 178 ng g_{dw}^{-1} h^{-1}) were higher.

SQT emissions were substantial compared to ISOP and MT emissions in all trees in Hyytiälä. The most noteworthy thing is that SQT emission rates greatly increase at the end of a growing season both in 2019 and 2021 (Fig. 4). For tree SF 2021, the emission rates increased a lot and the highest rates reached 3 µg g_{dw}^{-1} h^{-1} (Fig. A1). The emissions followed the typical diurnal variation with highest emission in the afternoon and lowest during the night (Fig. 5). The main identified SQT was β-farnesene, but significant fraction of the SQTs remained unidentified (Table 2). One of the major unidentified SQTs was tentatively identified as α-farnesene.

3.1.2 Emission rates at Pallas, northern Finland

At Pallas one big tree was measured with the in-situ TD-GC-MS in April-August 2020 (NF 2020) and two additional big trees were measured using adsorbent tubes in July 2020, one of them was growing by the roadside (NF 2020R) and the other deeper in the forest (NF 2020F). In these additional measurements only the new growth was measured.

Average emission rates of ISOP, MTs and SQTs from the main tree (NF 2020) were 7, 135 and 230 ng g_{dw}^{-1} h^{-1}, respectively. At the time of high emissions, in summer, SQTs were the most significant compounds group emitted (Table 2 and Fig. 4), although in spring when the emissions were quite low, MTs dominated. Diurnal variations of all emitted compounds followed the variations of temperature, as expected (Fig. 5). Significant emissions of MTs and SQTs were detected also during nighttime, while emissions of ISOP and MBO decreased close to or below detection limits. ISOP and MBO emissions are known to be light dependent (Harley et al., 1998; Guenther et al., 1997) and even though there is midnight sun at this sub-Arctic site in summer, PAR decreased down to <10 µmol s^{-1} m^{-2} in the middle of the night.

The emissions of the main tree and two additional trees with new growth measurements differed a lot. The additional tree growing deeper in the forest (NF 2020F) emitted about 10 times more MTs than the other two trees, and also SQT emission rates were higher (Table 2). We have no explanation for this difference. ISOP emissions were very low all the time from all trees. The branches were searched for possible diseases, but nothing was found. However, all three trees in Pallas had quite similar emission composition (Table 2). β-farnesene was the dominant SQT and other abundant compounds were α-pinene, β-pinene, limonene and Δ^3-carene.

https://doi.org/10.5194/acp-2022-478
Preprint. Discussion started: 28 July 2022

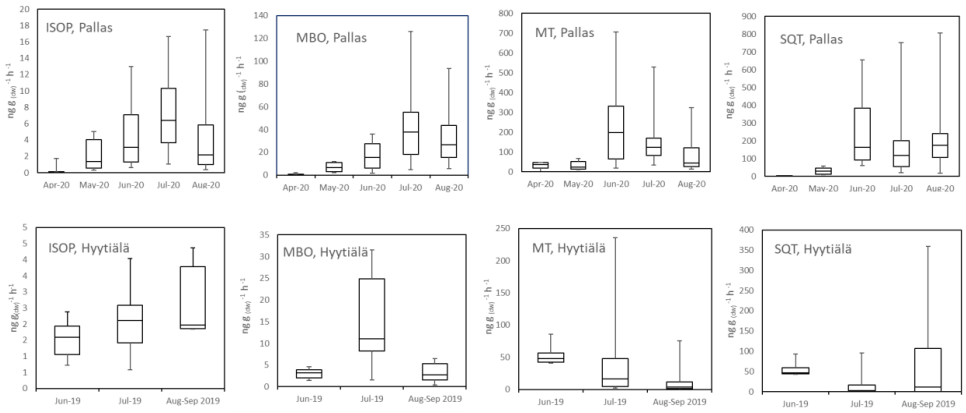

Fig. 4. Monthly mean box and whisker plots of ISOP, MBO, MT, and SQT calculated from daily mean emission rates of trees in Pallas in 2020 (NF 2020) and in Hyytiälä in 2019 (SF 2019). Boxes represent second and third quartiles and horizontal lines in the boxes median values. Whiskers show the highest and the lowest daily means.

https://doi.org/10.5194/acp-2022-478
Preprint. Discussion started: 28 July 2022

Table 2: Mean monthly emission potentials (30 °C) from the present study and from literature (ng $g^{-1}_{(dw)}$ h^{-1}). da=degraded in the analysis, na=not available. Van Meeningen et al. (2017) reported measurements from several heights, 1-2 m measurements are included here, since they best correspond to our measurements. For Norunda, Sweden, the height is 3 m and Järvselja, Estonia 16 m. β is the coefficient describing temperature dependence according to Eq. 3.

tree	tree age, years	time	β (MT)	β (SQT)	ISOP	MT	OMT	SQT	reference
NF2 2002	>80								this publication
67.25°N		April, 2002	0.1	0.17	481	394	133	0	
		May, 2002	0.1	0.17	2467	585	178	97	
		June, 2002	0.1	0.17	7138	1983	264	263	
NF 2020	>80								this publication
67.59°N		April, 2020	0.1	0.17	19	449	21	89	
		May, 2020	0.1	0.17	26	91	9	372	
		June, 2020	0.1	0.17	66	593	54	2282	
		July, 2020	0.1	0.17	76	390	148	1258	
		August, 2020	0.1	0.17	64	326	78	2719	
NF 2020 R (road side)	>80								this publication
adsorbent tubes. New growth only		July, 2020	0.1	0.17	5	190	60	96	
NF 2020 F (forest)	>80								this publication
adsorbent tubes. New growth only		July, 2020	0.1	0.17	12	2909	652	647	
SF 2011	40								Hakola et al. (2017)
61.51° N		April, 2011	0.1	0.17	0	64	12	da	
		May, 2011	0.1	0.17	115	25	5	da	
		June, 2011	0.1	0.17	3	47	13	da	
SF 2014	33-40								Hakola et al. (2017)
		May, 2014	0.1	0.17		88	6	da	
		June, 2014	0.1	0.17		39	11	da	
		July, 2014	0.1	0.17		87	10	da	
SF 2015	33-40								Hakola et al. (2017)
same tree as 2014		June, 2015	0.1	0.17	164	140	42	da	
		July, 2015	0.1	0.17	33	160	48	da	
		August, 2015	0.1	0.17	180	67	25	da	
SF 2019	33-40								this publication
		June, 2019	0.1	0.17	13	29	36	42	
		July, 2019	0.1	0.17	14	58	24	34	
		August, 2019	0.1	0.17	11	12	3	118	
		September, 2019	0.1	0.17		9	1	2333	
SF 2021	50								this publication
same tree as 2011		August, 2021	0.1	0.17	1	32	10	2173	
		September, 2021	0.1	0.17	0	24	7	13664	
SF 2021 B	50								this publication
adsorbent tubes		July, 2021	0.1	0.17	2063	284	69	3243	
		August, 2021	0.1	0.17	1181	53	5	114	
SF2 2001	>100								Hakola et al. (2003)
adsorbent tubes		spring 2001	0.1	0.17	488	409	55	8	
60.28°N		summer 2001	0.1	0.17	946	636	52	225	
		autumn 2001	0.1	0.17	635	228	8	59	
Järvselja, Estonia	big tree								Bourtsoukidis et al. (2014a)
58.27°N		autumn 2012	0.10±0.02	0.13±0.04	low	540		113	
Taunus mountains	60-80								Bourtsoukidis et al. (2014b)
Germany		spring 2011	0.14±0.02	0.09±0.01	low	2837		534	
50.22°N		summer 2011	0.12±0.02	0.12±0.02	low	978		353	
		autumn 2011	0.08±0.01	0.11±0.01	low	356		176	
Ljubljana, Slovenia, 46°04	54	Apr-May			310	1170		500	van Meeningen et al. (2017)
Grafrath, Germany, 48°18	51-53	June			640	1600		100	van Meeningen et al. (2017)
Taastrup, Denmark, 55°40	43-45	July			510	1960		330	van Meeningen et al. (2017)
Hyltemossa, Sweden, 56°06	30	July			430	1250		340	van Meeningen et al. (2017)
Skoagaryd, Sweden, 58°23	53	Oct			110	290		n.d.	van Meeningen et al. (2017)
Norunda, Sweden, 60°05	119	June			3790	1250		340	van Meeningen et al. (2017)
Piikkiö, Finland, 60°23	49	July			100	1470		170	van Meeningen et al. (2017)

https://doi.org/10.5194/acp-2022-478
Preprint. Discussion started: 28 July 2022

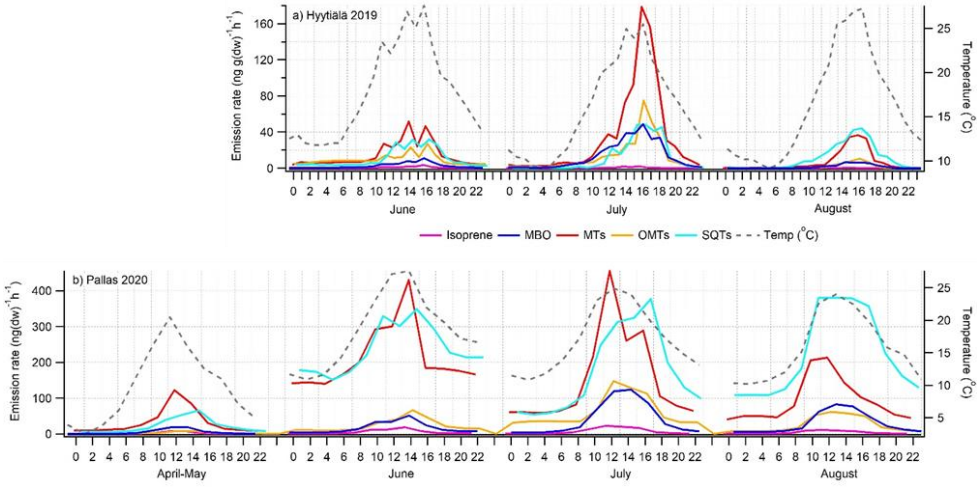

Fig. 5 Mean diurnal variations of isoprene, MBO, MTs, OMTs and SQTs in a) Hyytilä 2019 and b) Pallas 2020 together with the temperature in the enclosure.

Table 3: Contributions (%) of the most abundant compounds in the emissions of Norway spruce in Northern and Southern Finland trees. The empty cells means the compound was not detected.

	SF 2019	SF 2019	SF 2019	SF 2021	SF 2021	SF 2021B	SF2021B	NF 2020	NF 2020	NF 2020	NF 2020	NF 2020	NF 2020F	NF 2020R
	June	July	Aug	Aug	Sep	July	Aug	April	May	June	July	Aug	July	July
isoprene	1					72	85		3	1	2	1		
MBO	12	18	4	1		2	4	1	9	3	10	8		
MT														
α-pinene	7	4	3	1		2	2	13	16	11	10	5	15	14
β-pinene	5	3	1			1		10	3	7	4	3	12	7
camphene	2	4	3			1		4	6	4	5	2	14	13
carene	4	2				2		14	4	6	3	4	20	14
limonene	16	32	12	1		1		17	7	7	5	5	10	11
myrcene	1	2	1	1		1		25	2	4	2	2		
β-phellandrene								7	2	2	2	1		
sabinene	1	1	1						1	1	1			
terpinolene								3	1	1	0	1	1	2
MT total	36	48	21	4		9	3	93	43	43	32	24	72	61
OMT														
1,8-cineol	16	14	5	1				1	1		3	1	8	7
linalool	3	3		1		2		2		2	5	4	2	6
bornylacetate		1				n.a.	n.a.	1	1	2	4	1	6	5
OMT total	19	18	5	1		2		3	3	5	12	6	16	18
SQT														
iso-longifolene					24									
β-farnesene	17	7	26	46		11	4	1	18	35	35	41	11	20
β-caryophyllene	10	7												
a-humulene					21									
unidentifies SQTs	4	1	43	47	54	5	3	1	23	13	9	19		
SQT total	32	15	69	93	100	16	7	2	41	48	44	61	11	20
emission (ng $g_{(dw)}^{-1}$ h^{-1}	53	79	38	210	841	2082	499	36	68	474	449	452	1721	144
number of measureme	144	392	326	193	109	23	10	46	74	246	468	297	10	10

https://doi.org/10.5194/acp-2022-478
Preprint. Discussion started: 28 July 2022

3.2 Comparison of Norway spruce emission potentials

3.2.1. Sources of data for Norway spruce emission potentials

To study the variations of the Norway spruce VOC emission potentials and factors affecting them, emission potentials at 30 °C from earlier literature and from new measurements presented in the previous section were collected (Table 2). First, it includes data obtained in Hyytiälä during campaigns in 2011, 2014, and 2015 (Hakola et al., 2017), as well as the new data from 2019 and 2021, described above, and two older data sets; one from Sodankylä, northern Finland and one from Järvenpää, southern Finland.

On top of emission rates measured by our group, we included results from van Meeningen et al. (2017) and Bourtsoukidis et al. (2014a, 2014b). van Meeningen et al. (2017) reported isoprenoid emissions rates of Norway spruce at seven different sites, distributed from Ljubljana (46°06 N), Slovenia, to Piikkiö (60°23 N), Finland, to study the effect of latitude. Bourtsoukidis et al. (2014b) reported spruce emission measurements from Germany in Taunus Observatory on top of Kleiner Feldberg. There, the dominant spruce trees reached a maximum height of about 17 m, but the measurements were conducted at 2 m height at the edge of the forest. Bourtsoukidis et al. (2014a) measured spruce emissions also in Estonia during autumn. The age of the tree is not mentioned, but the measurements were conducted at 16 m height, so it is labeled as a “big tree”.

The mean of all emission potentials of Norway spruce emissions measured during summer months (June-August) at different sites presented (Table 2) was 760, 630 and 870 ng g_{dw}^{-1} h^{-1} for ISOP, MTs, and SQTs, respectively, but the variation between the trees and sites was very high. These are discussed in more details in the following subsections.

3.2.2. Variations in spruce BVOC emission potentials

The compiled ISOP emissions potentials ranged from below detection limit to 7138 ng g_{dw}^{-1} h^{-1}. No clear link between the emissions potentials and the latitude, or the season could be observed, but none of the smaller trees investigated emitted ISOP. The trees with the largest emissions were NF2 2002, SF2 2001, and SF 2021B, in June and July. Their ISOP emission potentials were larger than the one reported by van Menningen et al. (2017), except for the tree in Norunda (60°23N), Sweden. While this could indicate that ISOP emission potentials might be higher at higher latitudes, the trees in Pallas (NF 2020, NF 2020R, NF 2020F) and in Hyytiälä (SF 2019, SF 2021) and reported by Bourtsoukidis et al. (2014a, 2014b) also exhibited low ISOP emission potentials. According to our observations, latitude is not a main driver for variations in emission potentials, which is also in accordance with van Menningen et al. (2017) who found only minimal differences in emission potentials between sites and across latitude. Van Menningen et al. (2017) studied the effects of branch height, the season and variation between years on observed emission pattern was also investigated. There were indications of potential influences of all three factors. However, due to different experimental setups between measurement campaigns, it was difficult to draw any robust conclusions. The effect of branch height has not been explicitly studied in our campaigns as only the lowest branches were measured.

3.2.3. Variation in MT emission potentials

https://doi.org/10.5194/acp-2022-478
Preprint. Discussion started: 28 July 2022

We found larger variations of MT emission potentials (9–2909 ng $g_{(dw)}^{-1}$ h^{-1}) compared to van Menningen et al. (2017) and Bourtsoukidis et al. (2014a, 2014b), again with no clear trend with changes in latitude. Even for the summer months (June to August), the variations were large (39–2909 ng g_{dw}^{-1} h^{-1}). Here, it seems that, in general, younger trees (less than 80 years old) had lower MT emission potentials (9 - 1960 ng $g_{(dw)}^{-1}$ h^{-1}), compared to older trees (91–2909 ng $g_{(dw)}^{-1}$ h^{-1}), with a large overlap of values. Whenever seasonal data is available, MT emission potentials were higher in spring and summer. This confirms the findings from Bourtsoukidis et al. (2014a), in which the highest MT (977.5±140.7 ng $g_{dw}^{-1}h^{-1}$) emission potentials were detected during spring with a decline towards autumn.

3.2.4. Variation in OMT emission potentials

Studies from other groups have not reported OMT emission potentials separately. In our studies emission potentials of OMTs have ranged from below detection limit to 19 ng g_{dw}^{-1} h^{-1}. The largest emission potentials were found in July for the trees NF 2020F, NF2 2002 and NF 2020.

3.2.5. Variation in SQT emission potentials

As was shown in Helin et al. (2020), the SQT measurements from our early campaigns in Hyytiälä in 2011 and 2014 were underestimated, since β-farnesene, usually the main SQT emitted from Norway spruce, was degraded during the analysis. The SQT emission potentials from 2011 and 2014 are therefore not shown in Table 2. The SQT emissions potentials based on the rest of our measurement campaigns varied between below detection limit and 13664 ng g_{dw}^{-1} h^{-1} (between 34 and 3243 ng g_{dw}^{-1} h^{-1} for the summer months). Bourtsoukidis et al. (2014a) reported highest SQT emission potentials in spring (352.9±56.1 ng g_{dw}^{-1} h^{-1}), declining towards autumn, similarly to MT emission potentials from the same study. All our measurements which continued until late summer/early autumn have different trends with increasing emission potentials towards the end of the growing season (Table 2). Table 4 shows the mean values of emission potentials of the trees measured in Finland (this study and older data) and the standard deviation between the trees are shown. We did not take into account the results by Bourtsoukidis et al. (2014 a,b) or van Meeningen et al. (2017), because the standardization was not done with same β values and the ages of the trees in the measurements by Bourtsoukidis et al. (2014a) was not reported.

3.2.6. Overall conclusions of the comparison

Van Meeningen et al. (2017) concluded that spruce isoprenoid emission is potentially more determined by genetic diversity than by adaptation to local growth conditions. This conclusion is holding up in view of the review done here, even though weak trends could be identified regarding the age and size of the trees.

Generally, we found that older trees (>80y) emit more isoprene and MT than younger trees (<80y,) However, age does not seem to affect SQT emissions. This is reflected in the full review presented here, where comparing mean values of all measured trees older than 80 years and younger than 80 years. The old trees were found to emit about ten times more ISOP and MTs than younger trees (Table 4), while SQT emissions do not seem to vary with the age of the tree. SQT emissions are often related to stress effects as has been suggested in many studies (e.g. Petterson, 2007; Kännaste et al., 2008; Niinemets Ü, 2010; Joutsensaari et al., 2015; Matsui and Koeduka, 2016).

https://doi.org/10.5194/acp-2022-478
Preprint. Discussion started: 28 July 2022

While we found some indication that smaller trees have lower emission potentials, all the small trees measured were growing in Hyytiälä, so this could also be due to the same genetic origin. Big trees can be divided into two groups: three trees growing in NF emitted considerable amounts of MTs and SQTs, but small amounts of isoprene (as also the trees measured in Estonia and Germany by Bourtsoukidis et al. (2014a, b) and big trees growing in SF and one growing in NF emitted additionally lots of isoprene.

Table 4: Mean values of emission potentials for the trees (> 80 years, <80 years) measured in Finland (this study and older data) and the standard deviation between the trees. Number of trees measured each season is given in parentheses. bdl=below detection limit, Na=not available

>80 years	ISOP	MT	OMT	SQT
spring (3)	700±740	390±111	80±72	110±120
summer (5)	1200±3900	1000±840	190±110	1100±1100
autumn (1)	910	140	7	90

<80 years	ISOP	MT	OMT	SQT
spring (3)	60	40	8	Na
summer (6)	370±710	90±60	30±10	
summer (2) SQT				1300±1100
autumn (2)	bdl	16±11	4±4	8000±8010

4. Impact of Norway Spruce emissions on aerosol formation and growth

Recognizing this observed large variability in spruce BVOC emissions (precursors for new particle formation processes), there is a need to test the consequences of this variability in simulations of aerosol formation. For Southern Finland (SF) spruce forest emission potentials obtained from Hyytiälä were used, while for Northern Finland (NF) emission potentials obtained from Pallas were used. As a comparison, simulations were also conducted using standard emission potentials for Needleleaf Evergreen Boreal Tree from MEGAN v2.1. Simulations were run first by including all measured compounds and then either MT or SQT emissions were set to zero to study relative impacts of MTs and SQTs.

The emission potentials used in the simulations are listed in Table 5. ISOP was excluded from model simulations, since previous measurements as well as the measurements presented in this paper show that the emission of ISOP from Norway spruce is negligible or very low most of the time. Furthermore, the emission factor for ISOP for Needleleaf Evergreen Boreal Tree in MEGAN is very high (600 µg m^{-2} h^{-1} for a one-sided LAI of 1 m^2 m^{-2}, Guenther et al., 2012),

https://doi.org/10.5194/acp-2022-478
Preprint. Discussion started: 28 July 2022

due to the high emission of ISOP from other tree species within the same plant functional type (Guenther, 2013). Additionally, the role of ISOP in aerosol formation and growth processes is unclear. ISOP has a small HOM yield (~0.01-0.03 %, Jokinen et al., 2015) and it has been suggested that it suppresses the formation of new particles (Kiendler-Scharr et al., 2009, 2012; Lee et al., 2016; McFiggans et al., 2019; Heinritzi et al., 2020). On the other hand, oxidation products of ISOP (e.g. IEPOX) have been proposed to promote the growth of existing new particles (D_p > 3 nm, e.g., Surratt et al., 2010; Lin et al., 2013), while others have found the growth of small particles (D_p > 3.2 nm) to be unaffected by the concentration of ISOP (Heinritzi et al., 2020).

Table 5. Emission potentials (µg m^{-2} h^{-1}) used in the simulations. MT = monoterpenes, including oxygen-containing monoterpenes, SQT = sesquiterpenes.

	Southern Finland, 2019[a]		Northern Finland, 2020[a]		MEGAN v2.1[b]	
	MT	SQT	MT	SQT	MT	SQT
April			72	13	290	48
May			15	56	290	48
June	14	17	97	342	290	48
July	32	81	81	189	290	48
August	10	66	61	408	290	48
Sept	13	384			290	48

[a]: The values have been converted from ng g_{dw}^{-1} h^{-1} (shown in Table 2) to µg m^{-2} h^{-1} assuming a specific (one-sided) leaf weight of 0.15 kg m^{-2}. [b]: Needleleaf Evergreen Boreal Tree, the values have been decreased by a factor of 5, accounting for the fact that emission factors in MEGAN are standardised to a one-sided LAI of 5 m^2 m^{-2}.

Our data indicates that the Norway spruce dominated forests, especially in Northern Finland, are expected to have much higher SQT emissions than predicted by the standard emission potentials for Needleleaf Evergreen Boreal Tree in MEGAN 2.1. On the other hand, the ISOP and MT emission potentials obtained from our measurements are lower than those used in MEGAN v2.1. This can have significant impacts on predictions of formation and growth of new particles as shown in our model simulations.

According to our modeling efforts, oxidation products of primary BVOC emissions from spruce contribute significantly more to aerosol processes in northern Finland than in southern Finland. In the simulations of southern Finland, the sum of organic compounds contributing to aerosol processes (OxOrg) is 65 % smaller when using the emission potentials obtained from Hyytiälä compared to when using emission factors from MEGAN (Fig 6a). Using either emission potentials obtained from Pallas or from MEGAN reached comparable results when simulating northern Finland (Fig. 6a). Simulations conducted with and without MTs and SQTs showed that SQTs are the main contributors to OxOrg production in both southern and northern Finland when emission potentials obtained from Hyytiälä and Pallas are used, while

https://doi.org/10.5194/acp-2022-478
Preprint. Discussion started: 28 July 2022

MTs are the main contributors when emission factors from MEGAN are instead used (Fig. 6a). The dominance of SQTs is also displayed in the formation rate of new particles (Fig 6b), number of newly produced particles (Fig 6c) and the rate at which they grow (Fig 6d).

It is possible that spruce SQT emissions have been underpredicted in earlier studies due to difficulties in the quantitative measurements of their emissions. Based on our model simulations, these SQT emissions may have strong impacts on the formation and growth of new particles. However, neither emissions nor atmospheric processes of SQTs are well described, and more research would be needed to better characterize their atmospheric impacts and role in the biosphere-atmosphere interactions especially at Northern latitudes.

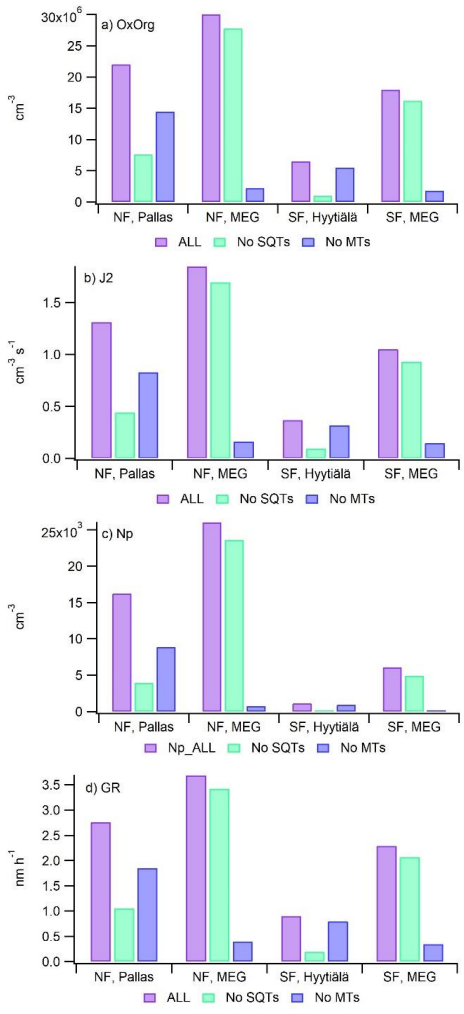

https://doi.org/10.5194/acp-2022-478
Preprint. Discussion started: 28 July 2022

Fig. 6. Results from the simulations of the formation and growth of new particles from the emissions of Norway spruce forests in Southern Finland (SF) and in Northern Finland (NF). Mean local emission potentials measured in Hyytiälä and Pallas or standard emission potentials for Needleleaf Evergreen Boreal Tree from MEGAN v2.1 (MEG) were used. a) sum of oxidation products of MT and SQT emissions contributing to aerosol processes (OxOrg), b) formation rate of neutral 2 nm sized clusters (J_2), c) number of new particles in the growing mode (Np), d) growth rate of newly formed particles (GR). All values are means of summer medians (June-August). Local environmental conditions are used in all simulations as described in the method section.

5. Conclusions

We studied VOC emissions from eight different Norway spruces growing in northern and southern Finland and reviewed the available VOC emission data of Norway spruces measured elsewhere. The outcome was that emissions were highly variable between individual trees. For MT and SQT ~80 times differences were found between the emission potentials of the highest and lowest emitting trees in summer. For isoprene the difference was even higher. No clear reason for the differences were found, but there were some indications of the impact of size/age of the trees and of the seasonality of emissions.

We found that none of the younger trees in Hyytiälä emitted isoprene, while one 50 year old tree growing in Hyytiälä was a strong isoprene emitter. This could perhaps indicate that young Norway spruce trees do not emit isoprene in contrast to older trees, but we cannot confirm this since all measured small trees were growing in Hyytiälä, thus the cause might be that the trees were of the same genetic origin. In addition, at other sites some big trees did not emit significant amounts of isoprene either. On average, older trees (>80 years) emitted about ten times more isoprene and MTs than younger ones (<80 years), but no clear difference was seen in SQT emissions. SQT emissions can be more related to stress effects as has been suggested in many studies (e.g. Petterson, 2007; Kännaste et al., 2008; Niinemets Ü, 2010; Joutsensaari et al., 2015; Matsui and Koeduka, 2016).

It is also significant that SQT emission rates greatly increased at the end of the growing season in all of the measurements conducted in Finland, but in the measurements by Bourtsoukidis et al., (2014b), high SQT emissions were measured during the early growing season. One tree (SF 2021) had an enormous increase in September when the highest emission rates reached 25 µg g^{-1}_{dw} h^{-1}. Increase of sesquiterpene emissions towards the late summer has also been seen in Scots pine branches (Tarvainen et al., 2005; Hakola et al., 2006).

With improved measurement methods in this study, we found much higher SQT emissions from Norway spruces than measured before and on average SQTs had higher emission potentials than isoprene and MTs. Due to difficulties in quantitative measurements, SQT emissions from other plant species may also be much higher than earlier thought. As shown here for Norway spruce, if the emission factors of SQTs are in reality higher than what is currently used in models, this may have very significant effects on predictions of aerosol dynamics, including the evolution of aerosol number size distribution via new particle formation and subsequent particle growth. Due to the high SOA formation potentials of SQTs

https://doi.org/10.5194/acp-2022-478
Preprint. Discussion started: 28 July 2022

(Griffin et al., 1999; Lee et al., 2006; Frosch et al., 2013; Mentel et al., 2013), the impact on SOA formation and mass could be even higher. Therefore, more studies should focus on quantifying the emission and atmospheric impacts of SQTs.

References:

Artaxo P., Hansson H-C, Andrea M.O., Bäck J., Alves E.G., Barbosa H.M.J., Bender F., Bourtsokoudis E., Carbone S., Chi J., Decesari S., Després V.R., Ditas F., Ezhova E., Fuzzi S., etc. Tropical and Boreal Forest- Atmosphere Interactions: A Review. Tellus B: Chemical and Physical Meteorology, 74(2022), 24–163. DOI: https:// doi.org/10.16993/tellusb.34 2022

Asm A., A. Wiedensohler, P. Laj, A.-M. Fjaeraa, K. Sellegri, W. Birmili, E. Weingartner, U. Baltensperger, V. Zdimal, N. Zikova, J.-P. Putaud, A. Marinoni, P. Tunved, H.-C. Hansson, M. Fiebig, N. Kivekäs, H. Lihavainen, E. Asmi, V. Ulevicius, P. P. Aalto, E. Swietlicki, A. Kristensson, N. Mihalopoulos, N. Kalivitis, I. Kalapov, G. Kiss, G. de Leeuw, B. Henzing, R. M. Harrison[18], D. Beddows, C. O'Dowd, S. G. Jennings, H. Flentje, K. Weinhold, F. Meinhardt, L. Ries, and M. Kulmala: Number size distributions and seasonality of submicron particles in Europe 2008–2009. Atmos. Chem. Phys., 11, 5505–5538, 2011. https://doi.org/10.5194/acp-11-5505-2011

Aurela M., Lohila A., Tuovinen J.-P., Hatakka J., Penttilä T. & Laurila T.: Carbon dioxide and energy flux measurements in four northern-boreal ecosystems at Pallas. Boreal Env. Res. 20: 455–473, 2015.

Berndt, T., Richters, S., Jokinen, T., Hyttinen, N., Kurtén, T., Otkjær, R. V., Kjaergaard, H. G., Stratmann, F., Herrmann, H., Sipilä, M., Kulmala, M., and Ehn, M.: Hydroxyl radical-induced formation of highly oxidized organic compounds, Nat. Commun., 7, 13677, https://doi.org/10.1038/ncomms13677, 2016.

Bourtsoukidis, E., Bonn, B., and Noe, S.: On-line field measurements of BVOC emissions from Norway spruce (Picea abies) at the hemiboreal SMEAR-Estonia site under autumn conditions, Boreal Environ. Res., 19, 153–167, 2014a.

Bourtsoukidis, E., Williams, J., Kesselmeier, J., Jacobi, S., and Bonn, B.: From emissions to ambient mixing ratios: online seasonal field measurements of volatile organic compounds over a Norway spruce-dominated forest in central Germany, Atmos. Chem. Phys., 14, 6495–6510, https://doi.org/10.5194/acp-14-6495-2014 , 2014b.

Bäck J., Aalto J., Henriksson M., Hakola H., He Q. and Boy M., 2012. Chemodiversity in terpene emissions in a boreal Scots pine stand. Biogeosciences, 9, 689–702.

Crounse John D., Lasse B. Nielsen, Solvejg Jørgensen, Henrik G. Kjaergaard,and Paul O. Wennberg: Autoxidation of Organic Compounds in the Atmosphere. Phys. Chem. Lett. 2013, 4, 20, 3513–3520, 2013. https://doi.org/10.1021/jz4019207

Ehn M., Kleist E. Junninen, H. Petaja, T. Lonn, G., Schobesberger S. Dal Maso M. Trimborn A., Kulmala M., Worsnop D. R., Wahner A., Wildt, J, Mentel Th F.: Gas phase formation of extremely oxidized pinene reaction products in chamber and ambient air. Atmos. Chem. Phys 12, 5113-5127, 2012. https://doi.org/10.5194/acp-12-5113-2012.

Ehn, M., Thornton, J. A., Kleist, E., Sipilä, M., Junninen, H., et al. 2014. A large source of low-volatility secondary organic aerosol. Nature 506, 476–79. DOI: *https://doi.org/10.1038/nature13032.*

Frosch, M., Bilde, M., Nenes, A., Praplan, A. P., Jurányi, Z., Dommen, J., Gysel, M., Weingartner, E., and Baltensperger, U.: CCN activity and volatility of caryophyllene secondary organic aerosol, Atmos. Chem. Phys., 13, 2283–2297, https://doi.org/10.5194/acp-13-2283-2013, 2013.

Guenther, A. B., Zimmerman, P. R., Harley, P. C., Monson, R. K., and Fall, R.: Isoprene and monoterpene emission rate variability: Model evaluation and sensitivity analyses, Journal of Geophysical Research, 98(D7), 12,609-12,627, 1993.

Guenther, A. B., Jiang, X., Heald, C. L., Sakulyanontvittaya, T., Duhl, T., Emmons, L. K., and Wang, X.: The Model of Emissions of Gases and Aerosols from Nature version 2.1 (MEGAN2.1): an extended and updated framework for modeling biogenic emissions, Geosci. Model Dev., 5, 1471-1492, https://doi.org/10.5194/gmd-5-1471-2012, 2012

Griffin, R. J., Cocker III, D. R., Flagan, R. C., and Seinfeld, J. H.: Organic aerosol formation from the oxidation of biogenic hydrocarbons, J. Geophys. Res., 104, 3555–3567, 1999.

Hakola H., Laurila T., Lindfors V., Hellén H. Gaman A. and Rinne J.: Variation of the VOC emission rates of birch species during the growing season. Boreal Environment Research, 6, 237-249, 2001.

Hakola, H., Tarvainen, V., Laurila, T., Hiltunen, V., Hellén, H. and Keronen, P.: Seasonal variation of VOC concentrations above a boreal coniferous forest. Atmos. Environ., 37, 1623-1634, 2003.

Hakola H., Tarvainen V., Bäck J., Rinne J., Ranta H., Bonn B., and Kulmala M., 2006. Seasonal variation of mono- and sesquiterpene emission rates of Scots pine. Biogeosciences, SRef-ID: 1726-4189/bg/2006-3-93, 93-101.

Hakola H., Tarvainen V., Praplan A.P., Jaars K., Hemmilä M., Kulmala M., Bäck J., Hellén H.: Terpenoid, acetone and aldehyde emissions from Norway spruce. Atmos. Chem. Phys., 17, 3357-3370, doi:10.5194/acp-17-3357-2017, 2017.

Hari, P. and Kulmala, M.: Station for measuring ecosystem-atmosphere relations (SMEAR II). Boreal Env. Res., *10*, 315-322, 2005.

Harley Peter, Verity Fridd-Stroud, James Greenberg, Alex Guenther, and Pérola Vasconcellos. Emission of 2-methyl-3-buten-2-ol by pines: A potentially large natural source of reactive carbon to the atmosphere. Journal of Geophysical Research, 103, 25 479-25 486, 1998.

Heinritzi, M., Dada, L., Simon, M., Stolzenburg, D., Wagner, A. C., Fischer, L., Ahonen, L. R., Amanatidis, S., Baalbaki, R., Baccarini, A., Bauer, P. S., Baumgartner, B., Bianchi, F., Brilke, S., Chen, D., Chiu, R., Dias, A., Dommen, J., Duplissy, J., Finkenzeller, H., Frege, C., Fuchs, C., Garmash, O., Gordon, H., Granzin, M., El Haddad, I., He, X., Helm, J., Hofbauer, V., Hoyle, C. R., Kangasluoma, J., Keber, T., Kim, C., Kürten, A., Lamkaddam, H., Laurila, T. M., Lampilahti, J., Lee, C. P., Lehtipalo, K., Leiminger, M., Mai, H., Makhmutov, V., Manninen, H. E., Marten, R., Mathot, S., Mauldin, R. L., Mentler, B., Molteni, U., Müller, T., Nie, W., Nieminen, T., Onnela, A., Partoll, E., Passananti, M., Petäjä, T., Pfeifer, J.,

Pospisilova, V., Quéléver, L. L. J., Rissanen, M. P., Rose, C., Schobesberger, S., Scholz, W., Scholze, K., Sipilä, M., Steiner, G., Stozhkov, Y., Tauber, C., Tham, Y. J., Vazquez-Pufleau, M., Virtanen, A., Vogel, A. L., Volkamer, R., Wagner, R., Wang, M., Weitz, L., Wimmer, D., Xiao, M., Yan, C., Ye, P., Zha, Q., Zhou, X., Amorim, A., Baltensperger, U., Hansel, A., Kulmala, M., Tomé, A., Winkler, P. M., Worsnop, D. R., Donahue, N. M., Kirkby, J., and Curtius, J.: Molecular understanding of the suppression of new-particle formation by isoprene, Atmos. Chem. Phys., 20, 11809–11821, https://doi.org/10.5194/acp-20-11809-2020, 2020.

Hellén Heidi , Arnaud P. Praplan, Toni Tykkä, Ilona Ylivinkka, Ville Vakkari, Jaana Bäck, Tuukka Petäjä, Markku Kulmala, and Hannele Hakola. Long-term measurements of volatile organic compounds highlight the importance of sesquiterpenes for the atmospheric chemistry of a boreal forest. Atmos. Chem. Phys., 18, 13839-13863, 2018. https://doi.org/10.5194/acp-18-13839-2018.

Hellén Heidi, Simon Schallhart, Arnaud P. Praplan, Toni Tykkä, Mika Aurela, Annalea Lohila, and Hannele Hakola. Sesquiterpenes dominate monoterpenes in northern wetland emissions. Atmos. Chem. Phys., 20, 7021–7034, 2020. https://doi.org/10.5194/acp-20-7021-2020

Hellén Heidi, Arnaud P. Praplan, Toni Tykkä, Aku Helin, Simon Schallhart, Piia P. Schiestl-Aalto, Jaana Bäck, and Hannele Hakola. Sesquiterpenes and oxygenated sesquiterpenes dominate the VOC (C_5–C_{20}) emissions of downy birches. Atmos. Chem. Phys., 21, 8045–8066, 2021. https://doi.org/10.5194/acp-21-8045-2021

Helin Aku, Hannele Hakola, and Heidi Hellén. Optimisation of a thermal desorption–gas chromatography–mass spectrometry method for the analysis of monoterpenes, sesquiterpenes and diterpenes. Atmos. Meas. Tech., 13, 3543–3560, 2020 https://doi.org/10.5194/amt-13-3543-2020.

Hirsikko, A., Laakso, L., Hõrrak, U., Aalto, P. P., Kerminen, V.- M., and Kulmala, M.: Annual and size dependent variation of growth rates and ion concentrations in boreal forest, Boreal Environ. Res., 10, 357–369, 2005Berndt, T., Richters, S., Jokinen, T., Hyttinen, N., Kurtén, T., Otkjær, R. V., Kjaergaard, H. G., Stratmann, F., Herrmann, H., Sipilä, M., Kulmala, M., and Ehn, M.: Hydroxyl radical-induced formation of highly oxidized organic compounds, Nat. Commun., 7, 13677, https://doi.org/10.1038/ncomms13677, 2016.

Häkkinen S. A. K., H. E. Manninen, T. Yli-Juuti, J. Merikanto, M. K. Kajos, T. Nieminen, S. D. D'Andrea, A. Asmi1, J. R. Pierce, M. Kulmala, and I. Riipinen. Semi-empirical parameterization of size-dependent atmospheric nanoparticle growth in continental environments. Atmos. Chem. Phys., 13, 7665–7682, 2013. www.atmos-chem-phys.net/13/7665/2013/

Jokinen Tuija , Torsten Berndt, Risto Makkonen, Veli-Matti Kerminen, Heikki Junninen, Pauli Paasonen, Frank Stratmann, Hartmut Herrmann, Alex B. Guenther, Douglas R. Worsnop, Markku Kulmala, Mikael Ehn, and Mikko Sipilä. Production of extremely low volatile organic compounds from biogenic emissions: Measured yields and atmospheric implications. PNAS 112 (23) 7123-7128, 2015. www.pnas.org/cgi/doi/10.1073/pnas.1423977112

Joutsensaari J., P. Yli-Pirilä, H. Korhonen, A. Arola, J. D. Blande, J. Heijari, M. Kivimäenpää, S. Mikkonen, L. Hao, P. Miettinen, P. Lyytikäinen-Saarenmaa, C. L. Faiola, A. Laaksonen, and J. K. Holopainen: Biotic stress accelerates formation of climate-relevant aerosols in boreal forests. Atmos. Chem. Phys., 15, 12139–12157, 10.5194/acp-15-12139-2015, 2015.

Kalliokoski Tuomo, Jaana Bäck, Michael Boy, Markku Kulmala, Nea Kuusinen, Annikki Mäkelä, Kari Minkkinen, Francesco Minunno, Pauli Paasonen, Mikko Peltoniemi, Ditte Taipale, Lauri Valsta, Anni Vanhatalo, Luxi Zhou, Putian Zhou and Frank Berninger. Mitigation Impact of Different Harvest Scenarios of Finnish Forests That Account for Albedo, Aerosols, and Trade-Offs of Carbon Sequestration and Avoided Emissions. Front. For. Glob. Change 3:562044, 2020. doi: 10.3389/ffgc.2020.562044

Karl M., A. Guenther, R. Koble1, A. Leip, and G. Seufert. A new European plant-specific emission inventory of biogenic volatile organic compounds for use in atmospheric transport models. Biogeosciences, 6, 1059–1087, 2009.

Kerminen V.-M. and Kulmala M.: Analytical formulae connecting the 'real' and the 'apparent' nucleation rate and the nuclei number concentration for atmospheric nucleation events. Journal of Aerosol Science, *33*, 609-622, 2002.

Kiendler-Scharr, A., Wildt, J., Dal Maso, M., Hohaus, T., Kleist, E., Mentel, T. F., Tillmann, R., Uerlings, R., Schurr, U., and Wahner, A.: New particle formation in forests inhibited by isoprene emissions, Nature, 461, 381–384, https://doi.org/10.1038/nature08292, 2009.

Kiendler-Scharr, A., Andres, S., Bachner, M., Behnke, K., Broch, S., Hofzumahaus, A., Holland, F., Kleist, E., Mentel, T. F., Rubach, F., Springer, M., Steitz, B., Tillmann, R., Wahner, A., Schnitzler, J.-P., and Wildt, J.: Isoprene in poplar emissions: effects on new particle formation and OH concentrations, Atmos. Chem. Phys., 12, 1021–1030, https://doi.org/10.5194/acp12-1021-2012, 2012.

Komppula M.,S.-L. Sihto, H. Korhonen, H. Lihavainen, V.-M. Kerminen, M. Kulmala, and Y. Viisanen. New particle formation in air mass transported between two measurement sites in Northern Finland. Atmos. Chem. Phys., 6, 2811–2824, 2006. https://doi.org/10.5194/acp-6-2811-2006

Kürten Andreas, Anton Bergen, Martin Heinritzi, Markus Leiminger, Verena Lorenz, Felix Piel, Mario Simon, Robert Sitals, Andrea C. Wagner, and Joachim Curtius. Observation of new particle formation and measurement of sulfuric acid, ammonia, amines and highly oxidized organic molecules at a rural site in central Germany. Atmos. Chem. Phys., 16, 12793–12813, 2016. https://doi.org/10.5194/acp-16-12793-2016

Kännaste A., Vongvanich N., Borg-Karlson A.-L.;.Infestation by a Nalepella species induces emissions of a – and b-farnesenes, (-)-linalool and aromatic compounds in Norway spruce clones of different susceptibility to the large pine weevil. Arthropod-Plant Interactions, 31–41, 2008.

Kyrö E.-M., R. Väänänen, V.-M. Kerminen, A. Virkkula, T. Petäjä, A. Asmi, M. Dal Maso, T. Nieminen, S. Juhola, A. Shcherbinin, I. Riipinen, K. Lehtipalo, P. Keronen, P. P. Aalto, P. Hari, and M. Kulmala. Trends in new particle formation in eastern Lapland, Finland: effect of decreasing sulfur emissions from Kola Peninsula Atmos. Chem. Phys., 14, 4383–4396, 2014. https://doi.org/10.5194/acp-14-4383-2014

Lee, A., Goldstein, A. H., Keywood, M. D., Gao, S., Varutbangkul, V., Bahreini, R., Ng, N. L., Flagan, R. C., and Seinfeld, J.H.: Gas-phase products and secondary aerosol yields from the ozonolysis of ten different terpenes, J. Geophys. Res., 111, D07302, 2006. https://doi.org/10.1029/2005JD006437.

Lee, S.-H., Uin, J., Guenther, A. B., de Gouw, J. A., Yu, F., Nadykto, A. B., Herb, J., Ng, N. L., Koss, A., Brune, W. B., Baumann, K., Kanawade, V. P., Keutsch, F. N., Nenes, A., Olsen,

K., Goldstein, A., and Ouyang, Q.: Isoprene suppression of new particle formation: Potential mechanisms and implications, J. Geophys. Res., 121, 14621–14635, https://doi.org/10.1002/2016JD024844, 2016.

Lehtinen K.E.J., M. Dal Maso, M. Kulmala, V.-M. Kerminen: Estimating nucleation rates from apparent particle formation rates and vice versa: Revised formulation of the Kerminen–Kulmala equation. Journal of Aerosol Science, 38, 988-994, 2007.

Lin, Y. H., Zhang, H., Pye, H. O. T., Zhang, Z., Marth, W. J., Park, S., Arashiro, M., Cui, T., Budisulistiorini, S. H., Sexton, K. G., Vizuete, W., Xie, Y., Luecken, D. J., Piletic, I. R., Edney, E. O., Bartolotti, L. J., Gold, A., and Surratt, J. D.: Epoxide as a precursor to secondary organic aerosol formation from isoprene photooxidation in the presence of nitrogen oxides, P. Natl. Acad. Sci. USA, 110, 6718–6723, https://doi.org/10.1073/pnas.1221150110, 2013.

Lohila A., Penttilä T., Jortikka S., Aalto T., Anttila P., Asmi E., Aurela M., Hatakka J., Hellén H., Henttonen H., Hänninen P., Kilkki J., Kyllönen K., Laurila T., Lepistö A., Lihavainen H., Makkonen U., Paatero J., Rask M., Sutinen R., Tuovinen J.-P., Vuorenmaa J. & Viisanen Y.: Preface to the special issue on integrated research of atmosphere, ecosystems and environment at Pallas. Boreal Env. Res. 20: 431–454, 2015.

Matsui, K and Koeduka, T.: Green Leaf Volatiles in Plant Signaling and Response, in: Lipids in Plant and Algae Development, edited by: Nakamura, Y. and Li-Beisson, Y., Springer International Publishing, 427–443, https://doi.org/10.1007/978-3-319-25979-6_17, 2016

McFiggans, G., Mentel, T. F., Wildt, J., Pullinen, I., Kang, S., Kleist, E., Schmitt, S., Springer, M., Tillmann, R., Wu, C., Zhao, D., Hallquist, M., Faxon, C., Le Breton, M., Hallquist, Å. M., Simpson, D., Bergström, R., Jenkin, M. E., Ehn, M., Thornton, J. A., Alfarra, M. R., Bannan, T. J., Percival, C. J., Priestley, M., Topping, D., and Kiendler-Scharr, A.: Secondary organic aerosol reduced by mixture of atmospheric vapours, Nature, 565, 587–593, https://doi.org/10.1038/s41586-018-0871-y, 2019.

Mentel Th. F., E. Kleist S. Andres, M. Dal Maso, T. Hohaus, A. Kiendler-Scharr, Y. Rudich, M. Springer, R. Tillmann, R. Uerlings A., Wahner and J. Wildt: Secondary aerosol formation from stress-induced biogenic emissions and possible climate feedbacks. Atmos. Chem. Phys., 13, 8755–8770, 2013. https://doi.org/10.5194/acp-13-8755-2013.

Mutzel Anke, Laurent Poulain, Torsten Berndt, Yoshiteru Iinuma, Maria Rodigast, Olaf Böge, Stefanie Richters, Gerald Spindler, Mikko Sipilä, Tuija Jokinen, Markku Kulmala, Hartmut Herrmann: Highly Oxidized Multifunctional Organic Compounds Observed in Tropospheric Particles: A Field and Laboratory Study. Environmental Science & Technology, *49*, 7754-7761, 2015. https://doi.org/10.1021/acs.est.5b00885

Niinemets Ü.; Responses of forest trees to single and multiple environmental stresses from seedlings to mature plants: Past stress history, stress interactions, tolerance and acclimation. Forest ecology and management 260 1623-1639, 2010.

Nölscher A.C., Bourtsoukidis E., Bonn B., Kesselmeier J., Lelieved J. and Williams J.: Seasonal measurements of total OH reavtivity emission rates from Norway spruce in 2011. Biogeosciences, 10, 4241-4257, 2013. https://doi.org/10.5194/bg-10-4241-2013, 2013.

Paasonen P., T. Nieminen, E. Asmi, H. E. Manninen, T. Petäjä, C. Plass-Dülmer, H. Flentje, W. Birmili, A. Wiedensohler, U. Hõrrak, A. Metzger, A. Hamed, A. Laaksonen, M. C. Facchini, V.-M. Kerminen, and M. Kulmala: On the roles of sulphuric acid and low-volatility organic vapours in the initial steps of atmospheric new particle formation. Atmos. Chem. Phys., 10, 11223–11242, 2010. https://doi.org/10.5194/acp-10-11223-2010

Pan, Y., Birdsey, R.A., Phillips, O.L., Jackson, R.B., 2013. The structure, distribution, and biomass of the world's forests. Annu. Rev. Ecol. Evol. Syst., 44, 593–622. DOI: https://doi.org/10.1146/annurev-ecolsys-110512-135914

Praplan Arnaud P., Toni Tykkä, Dean Chen, Michael Boy, Ditte Taipale, Ville Vakkari, Putian Zhou, Tuukka Petäjä, and Heidi Hellén: Long-term total OH reactivity measurements in a boreal forest. Atmos. Chem. Phys., 19, 14431–14453, 2019. https://doi.org/10.5194/acp-19-14431-2019

Praplan Arnaud P., Toni Tykkä, Simon Schallhart, Virpi Tarvainen, Jaana Bäck, and Heidi Hellén: OH reactivity from the emissions of different tree species: investigating the missing reactivity in a boreal forest. Biogeosciences, 17, 4681–4705, 2020. https://doi.org/10.5194/bg-17-4681-2020

Petäjä T., R. L. Mauldin, III, E. Kosciuch, J. McGrath, T. Nieminen, P. Paasonen, M. Boy, A. Adamov, T. Kotiaho, and M. Kulmala. Sulfuric acid and OH concentrations in a boreal forest site. Atmos. Chem. Phys., 9, 7435–7448, 2009. https://doi.org/10.5194/acp-9-7435-2009

Petterson Marie: Stress related emissions of Norway spruce plants. Licentiate thesis, KTH Royal Institute of Technology, Stockholm, ISBN 978-91-7178-644-9, 2007.

Rinne J., Bäck J. and Hakola H.. Biogenic volatile organic compound emissions from Eurasian taiga: current knowledge and future directions. Boreal Env. Res. 14: 807–826, 2009.

Roldin Pontus, Mikael Ehn, Theo Kurtén, Tinja Olenius, Matti P. Rissanen, Nina Sarnela, Jonas Elm, Pekka Rantala, Liqing Hao, Noora Hyttinen, Liine Heikkinen, Douglas R. Worsnop, Lukas Pichelstorfer, Carlton Xavier, Petri Clusius, Emilie Öström, Tuukka Petäjä, Markku Kulmala, Hanna Vehkamäki, Annele Virtanen, Ilona Riipinen and Michael Boy: The role of highly oxygenated organic molecules in the Boreal aerosol-cloud-climate system. Nature Comm. 10, 4370, 2019. https://doi.org/10.1038/s41467-019-12338-8.

Schallhart, S., Rantala, P., Kajos, M. K., Aalto, J., Mammarella, I., Ruuskanen, T. M., and Kulmala, M.: Temporal variation of VOC fluxes measured with PTR-TOF above a boreal forest, Atmos. Chem. Phys., 18, 815–832, 2018. https://doi.org/10.5194/acp-18-815-2018.

Sindelarova K., C. Granier, I. Bouarar, A. Guenther, S. Tilmes, T. Stavrakou, J.-F. Müller, U. Kuhn, P. Stefani, and W. Knorr: Global data set of biogenic VOC emissions calculated by the MEGAN model over the last 30 years. Atmos. Chem. Phys., 14, 9317–9341, 2014. https://doi.org/10.5194/acp-14-9317-2014

Soja, A. J., Tchebakova, N.M., French, N,H.F., Flannigan, M.D., Shugart, H.H., and co-authors, 2007, Climate-induced boreal forest change: Predictions versus current observations. Global and Planetary Change, 56, 274–296. DOI: https://doi.org/10.1016/j.gloplacha.2006.07.028

Surratt, J. D., Chan, A. W. H., Eddingsaas, N. C., Chan, M., Loza, C. L., Kwan, A. J., Hersey, S. P., Flagan, R. C., Wennberg, P. O., and Seinfeld, J. H.: Reactive intermediates revealed in secondary organic aerosol formation from isoprene, P. Natl. Acad. Sci. USA, 107, 6640–6645, https://doi.org/10.1073/pnas.0911114107, 2010.

Thum, T., T. Aalto, T. Laurila, M. Aurela, A. Lindroth, and T. Vesala: Assessing seasonality of biochemical CO_2 exchange model parameters from micrometeorological flux observations at boreal coniferous forest. Biogeosciences, 5, 1625–1639, 2008. https://doi.org/10.5194/bg-5-1625-2008.

Taipale Ditte, Veli-Matti Kerminen, Mikael Ehn, Markku Kulmala, and Ülo Niinemets. Modelling the influence of biotic plant stress on atmospheric aerosol particle processes throughout a growing season. Atmos. Chem. Phys., 21, 17389–17431, 2021. https://doi.org/10.5194/acp-21-17389-2021

Tarvainen V., H. Hakola, H. Hellén, J. Bäck, P. Hari, M. Kulmala. Temperature and light dependence of the VOC emissions of Scots pine. Atmos. Chem. Phys., 5, 6691-6718, 2005.

Tröstl Jasmin, Wayne K. Chuang, Hamish Gordon, Martin Heinritzi, Chao Yan, Ugo Molteni, Lars Ahlm, Carla Frege, Federico Bianchi, Robert Wagner, Mario Simon, Katrianne Lehtipalo, Christina Williamson, Jill S. Craven, Jonathan Duplissy, Alexey Adamov, Joao Almeida, Anne-Kathrin Bernhammer, Martin Breitenlechner, Sophia Brilke, Antònio Dias, Sebastian Ehrhart, Richard C. Flagan, Alessandro Franchin, Claudia Fuchs, Roberto Guida, Martin Gysel, Armin Hansel, Christopher R. Hoyle, Tuija Jokinen, Heikki Junninen, Juha Kangasluoma, Helmi Keskinen, Jaeseok Kim, Manuel Krapf, Andreas Kürten, Ari Laaksonen, Michael Lawler, Markus Leiminger, Serge Mathot, Ottmar M, Tuomo Nieminen, Antti Onnela, Tuukka Petäjä, Felix M. Piel, Pasi Miettinen, Matti P. Rissanen, Linda Rondo, Nina Sarnela Siegfried Schobesberger, Kamalika Sengupta, Mikko Sipilä, James N. Smith, Gerhard Steiner, Antònio Tomè, Annele Virtanen1, Andrea C. Wagner, Ernest Weingartner, Daniela Wimmer, Paul M. Winkler, Penglin Ye, Kenneth S. Carslaw, Joachim Curtius, Josef Dommen, Jasper Kirkby, Markku Kulmala, Ilona Riipinen, Douglas R. Worsnop, Neil M. Donahue and Urs Baltensperger: The role of low-volatility organic compounds in initial particle growth in the atmosphere. Nature 533, 527, 2016. https://doi.org/10.1038/nature18271

Yang Yudong, Shao Min, Wang, Xuemei, Noelscher, Anke C., Kessel Stephan, Guenther Alex, Williams Jonathan. Towards a quantitative understanding of total OH reactivity: A review. Atmos. Env. 134, 147-161, 2016. DOI 10.1016/j.atmosenv.2016.03.010

Yli-Juuti, T., T. Nieminen, A. Hirsikko, P.P. Aalto, E. Asmi, and co-authors. Growth rates of nucleation mode particles in Hyytiälä during 2003−2009: variation with particle size, season, data analysis method and ambient conditions. Atmos Chem Phys, 11, 12865–12886, 2011. https://doi.org/10.5194/acp-11-12865-2011

Zhao et al., 2020 is actually Zhao et al., 2021: Zhao, D., Pullinen, I., Fuchs, H., Schrade, S., Wu, R., Acir, I.-H., Tillmann, R., Rohrer, F., Wildt, J., Guo, Y., Kiendler-Scharr, A., Wahner, A., Kang, S., Vereecken, L., and Mentel, T. F.: Highly oxygenated organic molecule (HOM) formation in the isoprene oxidation by NO3 radical, Atmos. Chem. Phys., 21, 9681–9704, https://doi.org/10.5194/acp-21-9681-2021, 2021.

Vana Marko, Kaupo Komsaare, Urmas Hõrrak, Sander Mirme, Tuomo Nieminen, Jenni Kontkanen, Hanna E. Manninen, Tuukka Petäjä, Steffen M. Noe and Markku Kulmala. Characteristics of new-particle formation at three SMEAR stations. Boreal Env. Res. 21: 345–362, 2016.

van Meeningen Ylva, Min Wang, Tomas Karlsson, Ana Seifert, Guy Schurgers, Riikka Rinnan, Thomas Holst. Isoprenoid emission variation of Norway spruce across a European latitudinal transect. Atmospheric Environment 170, 45-57, 2017. https://doi.org/10.1016/j.atmosenv.2017.09.045

https://doi.org/10.5194/acp-2022-478
Preprint. Discussion started: 28 July 2022

Atmospheric Chemistry and Physics Discussions

Acknowledgments: The financial support by the Academy of Finland projects (project no. 316151, 307957 and 337549) and Academy of Finland Postdoctoral Researcher grant (323255) are gratefully acknowledged. The authors thank Dr. Juho Aalto for determining the tree ages. the needles and Dr. Pavel Alekseychik (National Resources Institute Finland), for providing us the figure taken using a drone (Fig. 2).

APPENDIX 1

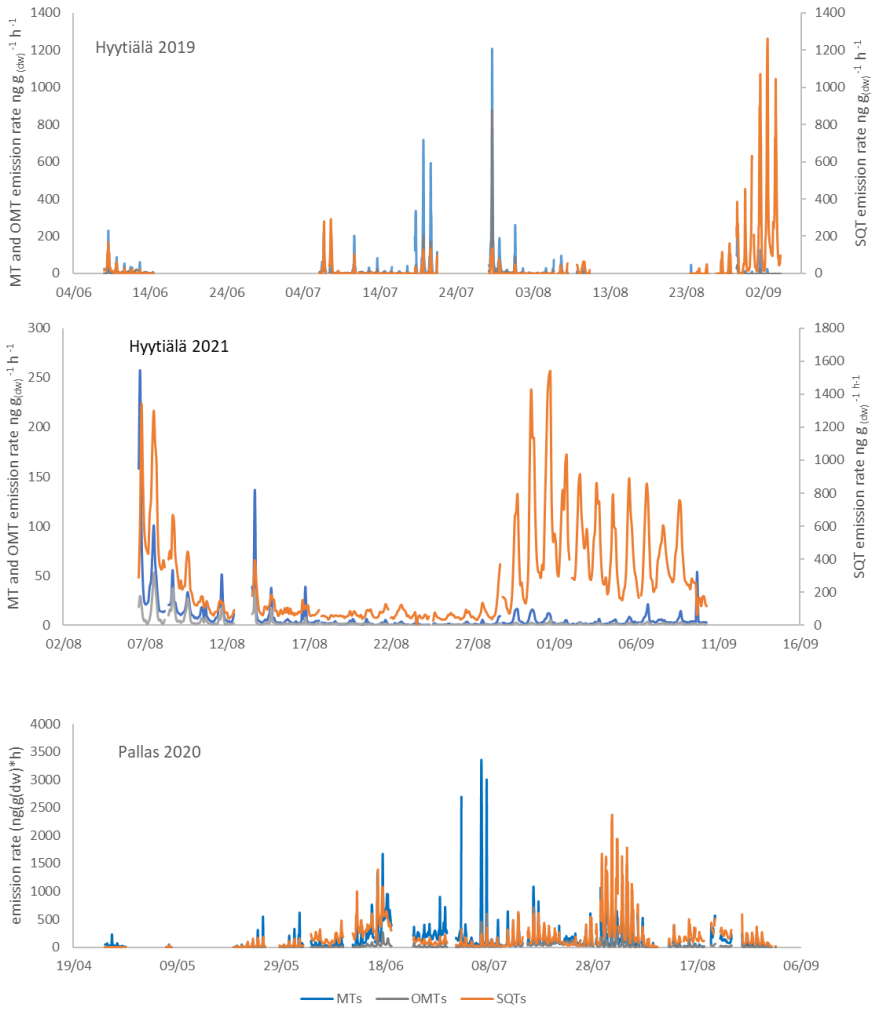

https://doi.org/10.5194/acp-2022-478
Preprint. Discussion started: 28 July 2022

Fig. A1 Monoterpene, oxygenated monoterpene and sesquiterpene emission rates in Hyytiälä and Pallas.

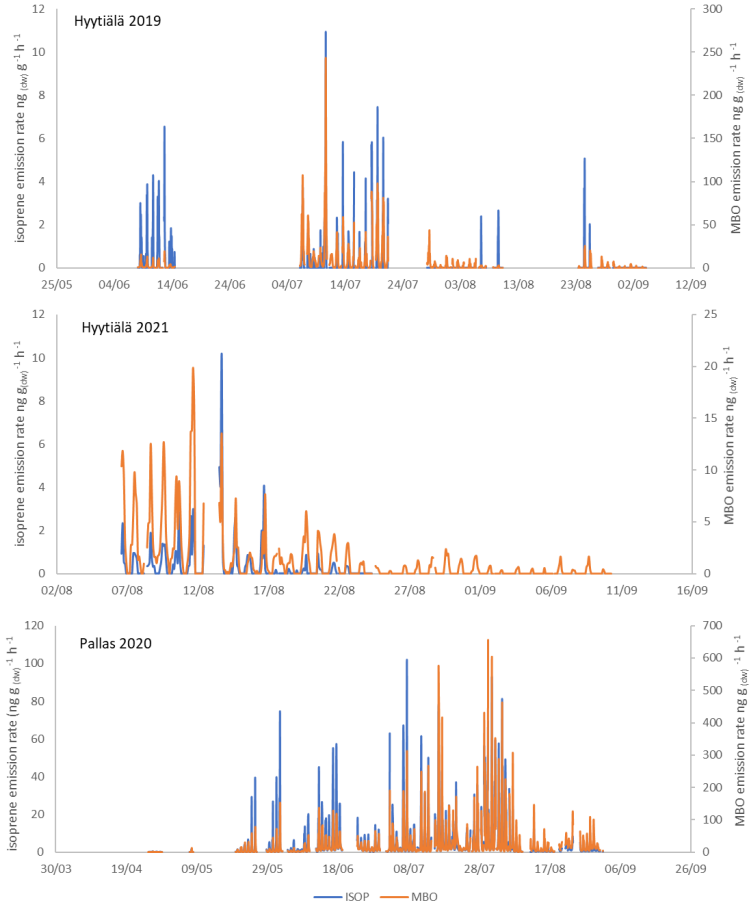

Fig. A2 Isoprene and MBO emission rates in Hyytiälä and Pallas